Protocol-Based SMC for Interval Type-2 Fuzzy Semi-Markovian Jumping Systems With Channel Fading

Wenhai Qi, *Senior Member, IEEE*, Ning Zhang, Ju H. Park, *Senior Member, IEEE*, Hak-Keung Lam, *Fellow, IEEE*, and Jun Cheng

***Abstract*—The sliding mode control (SMC) problem is studied for interval type-2 fuzzy semi-Markovian jumping systems subject to channel fading. To reduce the network burden, a dynamic event-triggered protocol is adopted to improve the transmission efficiency. A key feature is that the signal transmission is inevitably affected by fading phenomenon due to random noise and amplitude attenuation during the wireless communication. The main challenge lies in designing an appropriate fuzzy control scheme to achieve the reachability of the specified sliding region in line with channel fading. Under the common sliding surface, a fuzzy SMC law is constructed, which is related to the state signals affected by dynamic event-triggered protocol and channel fading. Then, by means of the boundary information of the global membership functions, sufficient conditions to ensure the stochastic stability of the underlying system, and the system states can be driven on the specified sliding region within a finite-time interval, which attenuates the influence of the channel fading. In the end, the tunnel diode circuit model is simulated to verify the proposed SMC strategy.**

***Index Terms*—Channel fading, interval type-2 fuzzy (IT2F), semi-Markovian jumping systems (S-MJSs), stochastic stability.**

I. Introduction

In MANY complex dynamical systems, the structure and parameters may change randomly due to sudden environmental disturbances and uncontrolled component failures. Markovian jumping systems (MJSs) are suitable to describe random switching characteristics caused by external factors [1], [2] and find wide applications, such as aerospace systems, macroeconomic models, and vehicle control systems [3], [4], [5], [6]. Although MJSs can describe the characteristics of multimodal switching in most practical systems, there still exist some constraints, resulting in inaccurate modeling. One of the main constraints is that the sojourn time (ST) of MJSs is a random variable with exponential distribution. Due to the memoryless property of exponential distribution, the system mode switching is only related to the previous mode. To eliminate this limitation, semi-Markovian jumping systems (S-MJSs) are introduced into the field of system control [7]. Compared with MJSs, the ST of submodes in S-MJSs follows more general distribution types and the transition rate (TR) among different modes is dependent on the ST, yielding a wider range of applications. In recent years, there have been many achievements in the research of S-MJSs [8], [9], [10], [11], [12], [13], [14].

As a typical fuzzy strategy, Takagi–Sugeno (T-S) fuzzy model is described by a series of "IF–THEN" rules, approximating arbitrary nonlinear systems with a set of linearized models in local scope, which makes nonlinear systems easier to analyze [15], [16], [17]. For example, a novel fuzzy sliding surface relating to the singularly perturbed parameter has been constructed to adapt the singularly perturbed systems characteristics for the first time, and the effective observer-based sliding mode controller has been designed for complex fuzzy systems [17]. Nowadays, type-1 fuzzy model has been widely adopted to model nonlinear systems. However, the membership function of type-1 fuzzy set is "exact," which has some limitations in dealing with parameter uncertainty. In order to make fuzzy sets with a stronger ability to handle the parameter uncertainty, the concept of type-2 fuzzy sets is introduced [18], [19]. Unlike type-1 fuzzy model, type-2 fuzzy model can better represent and deal with the system uncertainty, while the disadvantage is to increase the computational burden. As a special case of type-2 fuzzy model, interval type-2 fuzzy (IT2F) model not only retains the advantage of type-2 fuzzy model, but also reduces the computational complexity. Very recently, many researchers have paid more and more attention to IT2F model [20], [21], and successfully conducted in-depth research and generalization in fuzzy neural network control, dynamic trajectory, diagnostic fault, and other fields [22], [23], [24]. Due to its outstanding advantage, IT2F strategy has been successfully applied to MJSs

Manuscript received 16 November 2022; revised 27 February 2023; accepted 13 April 2023. Date of publication 18 April 2023; date of current version 1 November 2023. This work was supported in part by the National Natural Science Foundation of China under Grant 62073188, in part by the Natural Science Foundation of Shandong Province of China under Grant ZR2021MF083, and in part by the Postdoctoral Science Foundation of China under Grant 2022T150374. The work of Ju H. Park was supported by the National Research Foundation of Korea (NRF) through Korea government (Ministry of Science and ICT) under Grant 2019R1A5A8080290. *(Corresponding author: Ju H. Park.)*

Wenhai Qi and Ning Zhang are with the School of Engineering, Qufu Normal University, Rizhao 276826, China, and also with the School of Information Science and Engineering, Chengdu University, Chengdu 610106, China (e-mail: qiwhtanedu@163.com).

Ju H. Park is with the Department of Electrical Engineering, Yeungnam University, Kyongsan 38541, South Korea (e-mail: jessie@ynu.ac.kr).

Hak-Keung Lam is with the Department of Engineering, King's College London, WC2R 2LS London, U.K. (e-mail: hak-keung.lam@kcl.ac.uk).

Jun Cheng is with the College of Mathematics and Statistics, Guangxi Normal University, Guilin 541006, China (e-mail: jcheng6819@126.com).

Color versions of one or more figures in this article are available at https://doi.org/10.1109/TFUZZ.2023.3267777.

Digital Object Identifier 10.1109/TFUZZ.2023.3267777

and S-MJSs, including guaranteed cost control [13], fault detection [25], [26], and dissipativity [27], [28].

Sliding mode control (SMC) has been widely concerned because of its strong robustness to system parameter perturbations and external disturbances [29], [30]. In essence, SMC belongs to a special nonlinear control, the biggest feature of which is that the "structure" is not fixed, and the controller can be switched according to the current state signal, so that the system state can move to the equilibrium point along the preset sliding surface. A review of literature has witnessed the development of SMC theory, such as fuzzy control [2], [22], [23], [31], [32], MJSs [33], [34], and S-MJSs [9], [35], [36], [37]. Meantime, with the increasing diversity of wireless communication, the dynamical performance is largely restricted by the characteristics of wireless channels. In wireless communication, the transmitted signal is often affected by occlusion, reflection, refraction, and diffraction of various objects during the propagation process, forming a multipath signal component to arrive at the receiver. The signal components of different paths may have different phases and amplitudes, in which the received signal will be strengthened and weakened over a short time, resulting in channel fading [22], [23], [38], [39], [40]. Therefore, to improve the quality of wireless communication, it is necessary to study and analyze the transmission characteristics of channel fading.

Another issue is the triggered protocol. Based on the limited network bandwidth resources, an event-triggered protocol (ETP) has been developed to reduce the network burden [41], [42]. Compared with time-triggered protocol, the advantage of ETP lies in effectively reducing the transmitted number of sampled signals, so as to improve the utilization of computing and communication resources and avoid resource waste. However, it is worth noting that most of the previous research results focus on the static ETP [41], [42], that is, the parameter related to the triggered condition is time invariant. With the in-depth study of event-triggered rule, the dynamic ETP related to internal dynamic variable has been proposed to reduce the triggered frequency [22], [23], [43], [44], [45]. The introduction of dynamic variable makes the triggered policy related to system state in real time, further reducing the total amount of data transmission in the network transmission and maintaining the system stability. Nevertheless, under the framework of dynamic ETP, there is no relevant literature about SMC for IT2F S-MJSs with channel fading, which is one motivation of the current work.

Although some excellent results have emerged for IT2F S-MJSs, there are still some obvious limitations. The corresponding IT2F S-MJSs are investigated based on the framework of ideal network channels [13], [25], [27], in which it is difficult to satisfy this strict restriction in complicated communication networks. Moreover, the existing results for IT2F stochastic switching systems are studied in light of time-triggered protocol [13], [25], [26], [27] or static ETP [9], in which the amount of data transmission is greatly increased. The introduction of dynamic ETP brings some difficulties to SMC for IT2F S-MJSs. For IT2F S-MJSs, it is still a problem worthy of further study to design the dynamic ETP to reduce the burden of network communication. Therefore, how to design an appropriate dynamic event-triggered SMC law to achieve better dynamic performance for IT2F S-MJSs with channel fading is still an urgent problem to be solved, which motivates our study.

Inspired by the abovementioned motivations, this article studies the protocol-based SMC for IT2F S-MJSs with channel fading. The main contributions of this work include the following.

1) Compared with IT2F S-MJSs [13], [25], [27] in the presence of ideal network channels, the SMC problem is first studied for IT2F S-MJSs under the framework of channel fading.
2) Different from IT2F stochastic switching systems under time-triggered protocol [13], [25], [26], [27] or static ETP [9], the dynamic ETP is adopted to conserve the network resources efficiently, which can adjust the triggered threshold dynamically.
3) Based on the dynamic ETP, the channel fading, and the mismatched membership functions, an appropriate SMC strategy is proposed to ensure the stochastic stability of the underlying system and the reachability of the specified sliding region. At the same time, the minimum triggered interval is obtained to avoid Zeno behavior.

Notations: $\lambda_{\max}(X)$ and $\lambda_{\min}(X)$ denote the maximum and minimum eigenvalues of the corresponding matrix. $\mathbb{E}\{\cdot\}$ stands for the expectation operator.

II. Problem Formulation

A. System Description

Consider the IT2F S-MJSs with the αth rule

Rule α: IF $\xi_1(z(t))$ is Q_1^α and $\xi_2(z(t))$ is Q_2^α and $\cdots$ and $\xi_b(z(t))$ is Q_b^α, THEN

$$\begin{aligned}\dot{z}(t) = (A_\alpha(\upsilon_t) + \triangle A_\alpha(\upsilon_t, t))z(t) + B_\alpha(\upsilon_t)(u(t) \\ + \varphi_\alpha(z(t), \upsilon_t, t))\end{aligned} \tag{1}$$

where $z(t) \in \Re^n$ and $u(t) \in \Re^m$ stand for the system state and control input, respectively. $\xi_p(z(t))$ denote the premise variables and Q_p^α $(p = 1, 2, \ldots, b;\ \alpha = 1, 2, \ldots, \beta)$ are the fuzzy sets. $A_\alpha(\upsilon_t)$ and $B_\alpha(\upsilon_t)$ are the matrices with appropriate dimensions. $\triangle A_\alpha(\upsilon_t, t)$ is given as $\triangle A_\alpha(\upsilon_t, t) = L_\alpha(\upsilon_t)E_\alpha(\upsilon_t, t)U_\alpha(\upsilon_t)$, where $E_\alpha(\upsilon_t, t)$ satisfies $E_\alpha^T(\upsilon_t, t)E_\alpha(\upsilon_t, t) \le I$. $\varphi_\alpha(z(t), \upsilon_t, t)$ means the nonlinearity with $\|\varphi_\alpha(z(t), \upsilon_t, t)\| \le \pi_\alpha(\upsilon_t)\|z(t)\|$. The firing strength for the αth fuzzy rule is denoted by

$$\varpi_\alpha(z(t)) = [\underline{\varpi}_\alpha(z(t)), \bar{\varpi}_\alpha(z(t))]$$

where $\underline{\varpi}_\alpha(z(t)) = \prod_{p=1}^b \underline{\rho}_{Q_p^\alpha}(\xi_p(z(t))) \ge 0$, $\bar{\varpi}_\alpha(z(t)) = \prod_{p=1}^b \bar{\rho}_{Q_p^\alpha}(\xi_p(z(t))) \ge 0$, and $\underline{\rho}_{Q_p^\alpha}(\xi_p(z(t))) \le \bar{\rho}_{Q_p^\alpha}(\xi_p(z(t)))$ with $\bar{\rho}_{Q_p^\alpha}(\xi_p(z(t))) \in [0, 1]$ and $\underline{\rho}_{Q_p^\alpha}(\xi_p(z(t))) \in [0, 1]$ being the lower and upper grades of membership.

$\{\upsilon_t, \tau\}_{t\ge 0} := \{\upsilon_q, \tau_q\}_{q\in\mathbb{N}_{\ge 1}}$ denotes the semi-Markovian process (SMP) in $\mathcal{F} = \{1, 2, \ldots, c\}$, where $\{\upsilon_q\}_{q\in\mathbb{N}_{\ge 1}}$ is the ST between the $(q-1)$th and qth transitions and $\{\upsilon_q\}_{q\in\mathbb{N}_{\ge 1}}$ means the mode index at the qth transition with TR matrix

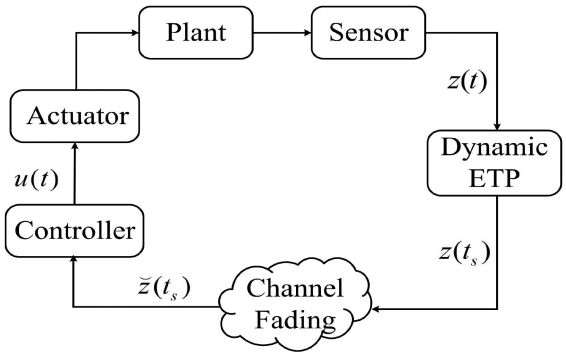

Fig. 1. System structure with dynamic ETP and channel fading.

$\Sigma(\tau)=\{\sigma_{\varrho\varsigma}(\tau)\}$ given by

$$\begin{cases}\Pr\{\upsilon_{q+1}=\varsigma,\tau_{q+1}\le\tau+d|\upsilon_q=\varrho,\tau_{q+1}>\tau\}\\ =\sigma_{\varrho\varsigma}(\tau)d+o(d),\varrho\neq\varsigma\\ \Pr\{\upsilon_{q+1}=\varsigma,\tau_{q+1}>\tau+d|\upsilon_q=\varrho,\tau_{q+1}>\tau\}\\ =1+\sigma_{\varrho\varsigma}(\tau)d+o(d),\varrho=\varsigma\end{cases}$$

where $\lim_{d\to0}o(d)/d=0$ with $d\ge0,\sigma_{\varrho\varsigma}(\tau)\ge0$ expresses the TR from ϱ to ς for $\varrho\neq\varsigma$, and $\sigma_{\varrho\varrho}(\tau)=-\sum_{\varsigma=1,\varrho\neq\varsigma}^{c}\sigma_{\varrho\varsigma}(\tau)<0$.

For the sake of notation, define $A_\alpha(\upsilon_t)\triangleq A_{\alpha\varrho}$, $B_\alpha(\upsilon_t)\triangleq B_{\alpha\varrho}$, and $\triangle A_\alpha(\upsilon_t,t)\triangleq\triangle A_{\alpha\varrho}(t)$. By fuzzy blending, one has the global model

$$\dot z(t)=\sum_{\alpha=1}^{\beta}\varpi_\alpha(z(t))[(A_{\alpha\varrho}+\triangle A_{\alpha\varrho}(t))z(t)+B_{\alpha\varrho}(u(t)+\varphi_{\alpha\varrho}(z(t),t))]\tag{2}$$

with

$$\varpi_\alpha(z(t))=\underline{\varpi}_\alpha(z(t))\underline{\phi}_\alpha(z(t))+\bar\varpi_\alpha(z(t))\bar\phi_\alpha(z(t))$$
$$\underline{\phi}_\alpha(z(t))+\bar\phi_\alpha(z(t))=1,\underline{\phi}_\alpha(z(t)),\bar\phi_\alpha(z(t))\in[0,1]$$

and $\sum_{\alpha=1}^{\beta}\varpi_\alpha(z(t))=1$, where $\underline{\phi}_\alpha(z(t))$ and $\bar\phi_\alpha(z(t))$ are the nonlinear functions that can capture the parameter uncertainty.

Remark 1: Compared with type-1 T-S fuzzy model [2], [3], [11], [15], [16], [32], IT2F model is adopted to describe S-MJSs, which makes up for the deficiency of modeling the parameter uncertainty in type-1 fuzzy strategy. In addition, IT2F model can effectively capture the parameter uncertainty by using the upper and lower membership functions, which greatly reduces the conservatism of the research results.

B. Dynamic ETP With Channel Fading

As shown in Fig. 1, the transmission of system state is regulated by the dynamic ETP to determine whether the state $z(t)$ can be released and transmitted to the controller. Let $t_s(s\in\mathbb{N})$ be the triggered instant, and the next triggered moment t_{s+1} is determined by the following dynamic ETP:

$$t_{s+1}=\inf\left\{t>t_s\middle|\frac{1}{\mu}\iota(t)+\vartheta z^T(t)\Psi_\varrho z(t)-\kappa^T(t)\Psi_\varrho\kappa(t)\le0\right\}\tag{3}$$

where $\mu>0$, $0<\vartheta<1$, and $\Psi_\varrho>0$ is the weight matrix. $\kappa(t)\triangleq z(t_s)-z(t)$ represents the error state between the latest released data $z(t_s)$ and the current data $z(t)$. Moreover, $\iota(t)$ is the dynamic variable satisfying the following:

$$\dot\iota(t)=-\eta\iota(t)+\vartheta z^T(t)\Psi_\varrho z(t)-\kappa^T(t)\Psi_\varrho\kappa(t)\tag{4}$$

with $\eta>0$ and $\iota(0)=\iota_0\ge0$.

Remark 2: For the dynamic ETP (3) and (4), the parameter $\mu>0$ reflects the involvement of dynamic variable $\iota(t)$. Obviously, as the parameter μ increases, the variable $\iota(t)$ becomes less and less involved. The parameter $0<\vartheta<1$ indicates the triggered tightness. The larger the value of ϑ, the larger the error $\kappa(t)$ tolerated by the system. This results in fewer packets being triggered. In addition, the parameter η stands for the decay rate of the variable $\iota(t)$. In general, choosing a smaller value can make its attenuation rate less than $\vartheta z^T(t)\Psi_\varrho z(t)-\kappa^T(t)\Psi_\varrho\kappa(t)$. Therefore, the parameters in dynamic ETP (3) and (4) can be selected appropriately to reduce the conservatism.

Lemma 1 [44]: Let $\mu>0$, $0<\vartheta<1$, $\Psi_\varrho>0$, $\eta>0$, and $\iota_0\ge0$. For $t\in\mathbb{R}_+$, the interval dynamic variable $\iota(t)$ in the event-triggered condition (3) with (4) satisfies $\iota(t)\ge0$.

Proof: For the dynamic ETP (3) and (4), one has

$$\dot\iota(t)+\eta\iota(t)=\vartheta z^T(t)\Psi_\varrho z(t)-\kappa^T(t)\Psi_\varrho\kappa(t)\ge\frac{-\iota(t)}{\mu\vartheta}$$

which means that $\iota(t)\ge\iota_0e^{-(\eta+\frac{1}{\mu\vartheta})t}\ge0$ with $\iota_0\ge0$. ■

Remark 3: Different from the static ETP [9], [32], [39], [41], [42], a dynamic ETP is adopted to better improve transmission efficiency. The triggered condition (3) contains a dynamic variable $\iota(t)$, the value of which can be dynamically adjusted according to the states $z(t)$ and $\kappa(t)$. According to Lemma 1, owing to the nonnegative term $\iota(t)$, the triggered interval between two consecutive triggered moments under dynamic ETP is not less than that under the static ETP. Therefore, the dynamic ETP can reduce the number of redundant data more effectively. In particular, when $\iota(t)\to0$, the dynamic ETP condition (3) will be transformed into the static ETP form.

Obviously, under the dynamic ETP, only part signals that meet the triggered condition (3) can be transmitted, and the limited network communication resources can be effectively utilized. However, due to the channel fading in the network transmission process, the signal $z(t_s)$ transmitted through the network communication channel may be affected. Therefore, the actual signal $\check z(t_s)$ transmitted to the controller from [22] is described as

$$\check z(t_s)=\delta(t_s)z(t_s)\tag{5}$$

where $\delta(t_s)\in[0,1]$ is a random variable that follows any probability density function with mathematical expectation $\bar\delta$ and variance $\tilde\delta$.

Remark 4: In the fading model (5), the random variable $\delta(t_s)\in[0,1]$ is adopted to describe the attenuation degree of the fading channel. Specifically, when $\delta(t_s)=1$, the actual transmitted signal cannot be affected by the channel fading,

normally transmitted to the controller. When $\delta(t_s)=0$, there is no transmitted signal.

Remark 5: In this article, the dynamic ETP (3) is adopted to reduce the network burden effectively. However, since the fading channel phenomenon is inevitable, this work constructs the fading channel model [22] on the basis of dynamic ETP, in which the dynamic ETP and the fading coefficient $\delta(t_s)\in[0,1]$ are taken into account. Obviously, this design makes the constructed controller more realistic. In addition, the actual signal received by the controller is the fading signal $\check{z}(t_s)$ described by the fading model (5), which also brings great challenges to the subsequent stability analysis.

C. SMC Law Design

Choose a common sliding function as

$$\gamma(t)=\mathcal{R}z(t) \tag{6}$$

where $\mathcal{R}$ is chosen such that $\mathcal{R}B_{\alpha\varrho}$ is nonsingular for $\forall\varrho\in\digamma$, $\alpha=1,2,\ldots,\beta$.

Remark 6: For the existing SMC schemes [2], [32], [33], a mode-dependent sliding surface is usually constructed. Although the mode switching is considered, it also brings some problems to the system performance. Frequent switching may result in unstable sliding motion. Therefore, a mode-independent sliding surface is constructed to avoid this problem, so as to effectively ensure the controller performance.

Based on the dynamic ETP and the channel fading, for $t\in[t_s,t_{s+1})$, the fuzzy sliding mode controller is constructed as

Rule ℓ: IF $o_1(\check{z}(t))$ is L_1^ℓ and $o_2(\check{z}(t))$ is L_2^ℓ and $\cdots$ and $o_f(\check{z}(t))$ is L_f^ℓ, THEN

$$u(t)=\mathcal{W}_{\ell\varrho}\check{z}(t_s)-\zeta_\varrho\|\check{z}(t_s)\|\text{sign}(\gamma(t)) \tag{7}$$

where the controller gain $\mathcal{W}_{\ell\varrho}$ and scalar ζ_ϱ will be designed later. $L_f^\ell(f=1,2,\ldots,g;\ell=1,2,\ldots,\hbar)$ represent the fuzzy sets of rule ℓ with premise variables $o_f(\check{z}(t))$. Considering the unknown membership functions, we reconstruct the membership functions as

$$\nu_\ell(\check{z}(t))=\underline{\nu}_\ell(\check{z}(t))\underline{\psi}_\ell(\check{z}(t))+\bar{\nu}_\ell(\check{z}(t))\bar{\psi}_\ell(\check{z}(t))$$
$$\underline{\psi}_\ell(\check{z}(t))+\bar{\psi}_\ell(\check{z}(t))=1,\underline{\psi}_\ell(\check{z}(t)),\bar{\psi}_\ell(\check{z}(t))\in[0,1]$$

where $\sum_{\ell=1}^{\hbar}\nu_\ell(\check{z}(t))=1$, $\underline{\nu}_\ell(\check{z}(t))=\prod_{f=1}^{g}\underline{\varepsilon}_{L_f^\ell}(o_f(\check{z}(t)))\geq 0$, $\bar{\nu}_\ell(\check{z}(t))=\prod_{f=1}^{g}\bar{\varepsilon}_{L_f^\ell}(o_f(\check{z}(t)))\geq 0$, and $\underline{\varepsilon}_{L_f^\ell}(o_f(\check{z}(t)))\leq\bar{\varepsilon}_{L_f^\ell}(o_f(\check{z}(t)))$ with $\bar{\varepsilon}_{L_f^\ell}(o_f(\check{z}(t)))\in[0,1]$ and $\underline{\varepsilon}_{L_f^\ell}(o_f(\check{z}(t)))\in[0,1]$ being the lower and upper grades of membership.

Then, the global fuzzy SMC law is inferred as

$$u(t)=\sum_{\ell=1}^{\hbar}\nu_\ell(\check{z}(t_s))\big[\mathcal{W}_{\ell\varrho}\check{z}(t_s)-\zeta_\varrho\|\check{z}(t_s)\|\text{sign}(\gamma(t))\big]. \tag{8}$$

Remark 7: It is noted that the signals triggered and transmitted by the dynamic ETP may also experience the fading phenomenon before reaching the controller through the network channel, which brings some challenges to the controller design. Unlike commonly designed controllers [5], [42], [43], [44], [45], the SMC law (8) is designed in terms of $\check{z}(t_s)$ and remains constant between the two triggered moments, making full consideration of fading phenomenon and dynamic ETP.

Therefore, the closed-loop system is obtained by combining (2), (5), and (8) that

$$\begin{aligned}\dot{z}(t)=\sum_{\alpha=1}^{\beta}\sum_{\ell=1}^{\hbar}\nu_{\alpha\ell}(z(t))\big[&(A_{\alpha\varrho}+\triangle A_{\alpha\varrho}(t)\\&+\delta(t_s)B_{\alpha\varrho}\mathcal{W}_{\ell\varrho})z(t)+\delta(t_s)B_{\alpha\varrho}\mathcal{W}_{\ell\varrho}\kappa(t)\\&+B_{\alpha\varrho}(\varphi_{\alpha\varrho}(z(t),t)-\zeta_\varrho\|\check{z}(t_s)\|\text{sign}(\gamma(t)))\big]\end{aligned} \tag{9}$$

where $\nu_{\alpha\ell}(z(t))=\varpi_\alpha(z(t))\nu_\ell(\check{z}(t_s))$.

Definition 1 ([1]): System (9) is said to be stochastically stable if for $\upsilon_0\in\digamma$ and $z_0\in\Re^n$, $\mathbb{E}\{\int_0^\infty\|z(t)\|^2dt\}<\infty$ holds.

The main objective is to construct an appropriate fuzzy SMC law (8) based on the dynamic ETP (3) to achieve the stochastic stability of IT2F S-MJSs and the reachability of the sliding dynamics with channel fading.

III. Main Results

An event-triggered SMC is studied for IT2F S-MJSs with channel fading. First, sufficient criteria are proposed to realize the stochastic stability of the underlying system (9). Then, the reachability condition of the sliding region is given. Finally, a lower bound on the triggered interval is shown in order to avoid Zeno behavior.

A. Stochastic Stability

Theorem 1: For given constants $\mu>0$, $0<\vartheta<1$, $\eta>0$, and $\theta>0$, system (9) is stochastically stable, if there exist scalars $\imath>0$, $\epsilon_1>0$, and $\epsilon_2>0$, and matrices $\mathcal{P}_\varrho>0$ and $\Psi_\varrho>0$ satisfying

$$B_{\alpha\varrho}^T\mathcal{P}_\varrho B_{\alpha\varrho}\leq\imath I \tag{10}$$

$$\sum_{\alpha=1}^{\beta}\sum_{\ell=1}^{\hbar}\nu_{\alpha\ell}(z(t))\Upsilon<0 \tag{11}$$

where

$$\Upsilon=\begin{bmatrix}\Upsilon_{11}&\bar{\delta}\mathcal{P}_\varrho B_{\alpha\varrho}\mathcal{W}_{\ell\varrho}&0\\*&\Upsilon_{22}&0\\*&*&\left(\frac{\theta}{\mu}-\eta\right)I\end{bmatrix}$$

$$\begin{aligned}\Upsilon_{11}=&\mathcal{P}_\varrho A_{\alpha\varrho}+A_{\alpha\varrho}^T\mathcal{P}_\varrho+\sum_{\varsigma=1}^{c}\bar{\sigma}_{\varrho\varsigma}\mathcal{P}_\varsigma+2\bar{\delta}\mathcal{P}_\varrho B_{\alpha\varrho}\mathcal{W}_{\ell\varrho}\\&+\epsilon_1^{-1}\mathcal{P}_\varrho L_{\alpha\varrho}L_{\alpha\varrho}^T\mathcal{P}_\varrho+\epsilon_1U_{\alpha\varrho}^TU_{\alpha\varrho}+\epsilon_2\mathcal{P}_\varrho\\&+2\epsilon_2^{-1}\imath(\pi_{\alpha\varrho}^2+\zeta_\varrho^2m(\bar{\delta}^2+\tilde{\delta}))I+(1+\theta)\vartheta\Psi_\varrho\\\Upsilon_{22}=&2\epsilon_2^{-1}\imath\zeta_\varrho^2m(\bar{\delta}^2+\tilde{\delta})I-(1+\theta)\Psi_\varrho.\end{aligned}$$

Proof: Select the following Lyapunov function:

$$\mathcal{V}(z(t),\varrho,\iota(t))=\mathcal{V}_1(z(t),\varrho)+\iota(t) \tag{12}$$

where $\mathcal{V}_1(z(t),\varrho)=z^T(t)\mathcal{P}_\varrho z(t)$.

For the weak infinitesimal operator of $\mathcal{V}_1(z(t),\varrho)$, it can be computed that

$$\begin{aligned}
&\Im\mathcal{V}_1(z(t),\varrho)\\
&=\lim_{d\to0^+}\frac{1}{d}\{\mathbb{E}[\mathcal{V}_1(z(t+d),\upsilon_{t+d})|\upsilon_t=\varrho]-\mathcal{V}_1(z(t),\varrho)\}\\
&=\lim_{d\to0^+}\frac{1}{d}\Bigg\{\mathbb{E}\Bigg[\sum_{\varsigma=1,\varrho\neq\varsigma}^{c}\Pr\{\upsilon_{q+1}=\varsigma,\tau_{q+1}\le\tau+d|\\
&\quad\upsilon_q=\varrho,\tau_{q+1}>\tau\}z^T(t+d)\mathcal{P}_\varsigma z(t+d)+\Pr\{\upsilon_{q+1}=\varsigma\\
&\quad\tau_{q+1}>\tau+d|\upsilon_q=\varrho,\tau_{q+1}>\tau\}z^T(t+d)\mathcal{P}_\varrho z(t+d)\Bigg]\\
&\quad-z^T(t)\mathcal{P}_\varrho z(t)\Bigg\}\\
&=\lim_{d\to0^+}\frac{1}{d}\Bigg\{\mathbb{E}\Bigg[\sum_{\varsigma=1,\varrho\neq\varsigma}^{c}\frac{\Pr\{\upsilon_{q+1}=\varsigma,\upsilon_q=\varrho\}}{\Pr\{\upsilon_q=\varrho\}}\\
&\quad\frac{\Pr\{\tau<\tau_{q+1}\le\tau+d|\upsilon_{q+1}=\varsigma,\upsilon_q=\varrho\}}{\Pr\{\tau_{q+1}>\tau+d|\upsilon_q=\varrho\}}z^T(t+d)\mathcal{P}_\varsigma z(t+d)\\
&\quad+\frac{\Pr\{\tau_{q+1}>\tau+d|\upsilon_q=\varrho\}}{\Pr\{\tau_{q+1}>\tau|\upsilon_q=\varrho\}}z^T(t+d)\mathcal{P}_\varrho z(t+d)\Bigg]\\
&\quad-z^T(t)\mathcal{P}_\varrho z(t)\Bigg\}\\
&=\lim_{d\to0^+}\frac{1}{d}\Bigg\{\mathbb{E}\Bigg[\sum_{\varsigma=1,\varrho\neq\varsigma}^{c}\frac{\chi_{\varrho\varsigma}(\mathcal{M}_\varrho(\tau+d)-\mathcal{M}_\varrho(\tau))}{1-\mathcal{M}_\varrho(\tau)}\\
&\quad z^T(t+d)\mathcal{P}_\varsigma z(t+d)+\frac{1-\mathcal{M}_\varrho(\tau+d)}{1-\mathcal{M}_\varrho(\tau)}z^T(t+d)\mathcal{P}_\varrho\\
&\quad z(t+d)\Bigg]-z^T(t)\mathcal{P}_\varrho z(t)\Bigg\}
\end{aligned}\tag{13}$$

where $\chi_{\varrho\varsigma}=\frac{\Pr\{\upsilon_{q+1}=\varsigma,\upsilon_q=\varrho\}}{\Pr\{\upsilon_q=\varrho\}}=\Pr\{\upsilon_{q+1}=\varsigma|\upsilon_q=\varrho\}$ stands for the probability intensity from ϱ to ς, and $\mathcal{M}_\varrho(\tau)$ is the cumulative distribution function.

For a given small scalar $d>0$, when $d\to0$, the expansion of Taylor formula for $z(t+d)$ is

$$z(t+d)=z(t)+\dot z(t)d+o(d).\tag{14}$$

Considering $\lim_{d\to0^+}\frac{1-\mathcal{M}_\varrho(\tau+d)}{1-\mathcal{M}_\varrho(\tau)}=1$, $\lim_{d\to0^+}\frac{\mathcal{M}_\varrho(\tau)-\mathcal{M}_\varrho(\tau+d)}{d(1-\mathcal{M}_\varrho(\tau))}=\sigma_\varrho(\tau)$, and $\sigma_{\varrho\varsigma}(\tau)=\sigma_\varrho(\tau)\chi_{\varrho\varsigma},\varrho\neq\varsigma$, where $\sigma_\varrho(\tau)$ denotes the TR of system switching from ϱ, we can obtain

$$\begin{aligned}
&\Im\mathcal{V}_1(z(t),\varrho)\\
&=2z^T(t)\mathcal{P}_\varrho\dot z(t)+\sum_{\varsigma=1}^{c}\bar\sigma_{\varrho\varsigma}z^T(t)\mathcal{P}_\varsigma z(t)
\end{aligned}$$

where $\bar\sigma_{\varrho\varsigma}=\mathbb{E}[\sigma_{\varrho\varsigma}(\tau)]=\int_0^\infty\sigma_{\varrho\varsigma}(\tau)\omega_\varrho(\tau)d\tau$, and $\omega_\varrho(\tau)$ represents the probability distribution function.

Furthermore,

$$\begin{aligned}
&\Im\mathcal{V}_1(z(t),\varrho,\iota(t))\\
&=\Im\mathcal{V}(z(t),\varrho)+\dot\iota(t)\\
&=2z^T(t)\mathcal{P}_\varrho\dot z(t)+\sum_{\varsigma=1}^{c}\bar\sigma_{\varrho\varsigma}z^T(t)\mathcal{P}_\varsigma z(t)-\eta\iota(t)\\
&\quad+\vartheta z^T(t)\Psi_\varrho z(t)-\kappa^T(t)\Psi_\varrho\kappa(t)\\
&=2\sum_{\alpha=1}^{\beta}\sum_{\ell=1}^{\hbar}\nu_{\alpha\ell}(z(t))z^T(t)\mathcal{P}_\varrho\big[(A_{\alpha\varrho}+\triangle A_{\alpha\varrho}(t)\\
&\quad+\delta(t_s)B_{\alpha\varrho}\mathcal{W}_{\ell\varrho})z(t)+\delta(t_s)B_{\alpha\varrho}\mathcal{W}_{\ell\varrho}\kappa(t)+B_{\alpha\varrho}(\varphi_{\alpha\varrho}(z(t),t)\\
&\quad-\zeta_\varrho\|\check z(t_s)\|\mathrm{sign}(\gamma(t)))\big]+\sum_{\varsigma=1}^{c}\bar\sigma_{\varrho\varsigma}z^T(t)\mathcal{P}_\varsigma z(t)\\
&\quad-\eta\iota(t)+\vartheta z^T(t)\Psi_\varrho z(t)-\kappa^T(t)\Psi_\varrho\kappa(t).
\end{aligned}\tag{15}$$

For $\epsilon_1>0$ and $\epsilon_2>0$, one has

$$\begin{aligned}
&2z^T(t)\mathcal{P}_\varrho\triangle A_{\alpha\varrho}(t)z(t)\\
&\le\epsilon_1^{-1}z^T(t)\mathcal{P}_\varrho L_{\alpha\varrho}L_{\alpha\varrho}^T\mathcal{P}_\varrho z(t)+\epsilon_1 z^T(t)U_{\alpha\varrho}^TU_{\alpha\varrho}z(t)
\end{aligned}\tag{16}$$

$$\begin{aligned}
&2z^T(t)\mathcal{P}_\varrho B_{\alpha\varrho}\tilde\varphi\\
&\le\epsilon_2 z^T(t)\mathcal{P}_\varrho z(t)+\epsilon_2^{-1}\tilde\varphi^TB_{\alpha\varrho}^T\mathcal{P}_\varrho B_{\alpha\varrho}\tilde\varphi\\
&\le\epsilon_2 z^T(t)\mathcal{P}_\varrho z(t)+2\epsilon_2^{-1}\imath\big[\pi_{\alpha\varrho}^2z^T(t)z(t)+\zeta_\varrho^2m\delta^2(t_s)\\
&\quad(z^T(t)z(t)+\kappa^T(t)\kappa(t))\big]
\end{aligned}\tag{17}$$

where $\tilde\varphi=\varphi_{\alpha\varrho}(z(t),t)-\zeta_\varrho\|\check z(t_s)\|\mathrm{sign}(\gamma(t))$.

From the condition (3), it can be obtained that for $t\in[t_s,t_{s+1})$

$$\frac{1}{\mu}\iota(t)+\vartheta z^T(t)\Psi_\varrho z(t)-\kappa^T(t)\Psi_\varrho\kappa(t)\ge0.\tag{18}$$

Combining (15)–(18), one has

$$\begin{aligned}
&\mathbb{E}\{\Im\mathcal{V}(z(t),\varrho,\iota(t))\}\\
&\le\sum_{\alpha=1}^{\beta}\sum_{\ell=1}^{\hbar}\nu_{\alpha\ell}(z(t))[z^T(t)(\mathcal{P}_\varrho A_{\alpha\varrho}+A_{\alpha\varrho}^T\mathcal{P}_\varrho\\
&\quad+2\bar\delta\mathcal{P}_\varrho B_{\alpha\varrho}\mathcal{W}_{\ell\varrho})z(t)+\epsilon_1^{-1}z^T(t)\mathcal{P}_\varrho L_{\alpha\varrho}L_{\alpha\varrho}^T\mathcal{P}_\varrho z(t)\\
&\quad+\epsilon_1z^T(t)U_{\alpha\varrho}^TU_{\alpha\varrho}z(t)+2\bar\delta z^T(t)\mathcal{P}_\varrho B_{\alpha\varrho}\mathcal{W}_{\ell\varrho}\kappa(t)\\
&\quad+\epsilon_2z^T(t)\mathcal{P}_\varrho z(t)+2\epsilon_2^{-1}\imath(\pi_{\alpha\varrho}^2+\zeta_\varrho^2m(\bar\delta^2+\tilde\delta))z^T(t)z(t)\\
&\quad+2\epsilon_2^{-1}\imath\zeta_\varrho^2m(\bar\delta^2+\tilde\delta)\kappa^T(t)\kappa(t)]+\left(\frac{\theta}{\mu}-\eta\right)\iota(t)\\
&\quad+(1+\theta)\vartheta z^T(t)\Psi_\varrho z(t)-(1+\theta)\kappa^T(t)\Psi_\varrho\kappa(t)\\
&\quad+\sum_{\varsigma=1}^{c}\bar\sigma_{\varrho\varsigma}z^T(t)\mathcal{P}_\varsigma z(t)
\end{aligned}$$

$$= \beth^T(t)\left[\sum_{\alpha=1}^{\beta}\sum_{\ell=1}^{\hbar}\nu_{\alpha\ell}(z(t))\Upsilon\right]\beth(t) \tag{19}$$

where $\beth(t) = [z^T(t), \kappa^T(t), \sqrt{\iota(t)}]^T$, and $\theta > 0$ is a constant.

According to (11), one has

$$\mathbb{E}\{\Im\mathcal{V}(z(t), \varrho, \iota(t))\} < 0.$$

Then, it can be obtained that

$$\mathbb{E}\{\Im\mathcal{V}(z(t), \varrho, \iota(t))\} \leq -\wp\|\beth(t)\|^2 < 0$$

where $\wp = \min\{\lambda_{\min}[-\Upsilon]\} > 0$.

Furthermore, we have $\mathbb{E}\{\int_0^\infty \|\beth(t)\|^2 dt\} \leq \frac{1}{\wp}\mathcal{V}(z_0, \varrho, \iota_0) < \infty$. Therefore, system (9) realizes the stochastic stability. ■

Remark 8: The constructed fuzzy SMC law (8) is based on the actual signal $\check{z}(t_s)$ transmitted to the controller, in which the dynamic ETP and the random attenuation of the signal by the channel fading are also considered. Moreover, the Lyapunov function constructed in Theorem 1 contains the dynamic variable $\iota(t)$, so the stability criterion is related to the dynamic ETP and the fading model parameters $\bar{\delta}$ and $\tilde{\delta}$. Obviously, the designed controller (8) can effectively reduce the influence of fading channel and realize the stochastic stability, which provides the basis for the subsequent solution of controller gain.

Since the product term $\nu_{\alpha\ell}(t) = \varpi_\alpha(z(t))\nu_\ell(\check{z}(t_s))$ is contained in condition (11), the membership functions of controller (8) and fuzzy system (2) are not exactly matched. In order to solve this product term, the global boundary information of $\nu_{\alpha\ell}(t)$ is adopted in Theorem 2 to obtain the stability criterion with relatively less conservatism.

Theorem 2: For given constants $\mu > 0$, $0 < \vartheta < 1$, $\eta > 0$, and $\theta > 0$, system (9) is stochastically stable, if there exist scalars $\imath > 0, \epsilon_1 > 0$, and $\epsilon_2 > 0$, and matrices $\bar{\mathcal{P}}_\varrho > 0$, $\bar{\Psi}_\varrho > 0$, $\bar{\Xi}_{\alpha\ell} \geq 0$, $\underline{\Xi}_{\alpha\ell} \geq 0$, and $\bar{\mathcal{W}}_{\ell\varrho}$ satisfying

$$\begin{bmatrix} -\imath I & B_{\alpha\varrho}^T \\ * & -\bar{\mathcal{P}}_\varrho \end{bmatrix} < 0 \tag{20}$$

$$\bar{\Upsilon} - \bar{\Xi}_{\alpha\ell} + \underline{\Xi}_{\alpha\ell} + \sum_{i=1}^{\beta}\sum_{j=1}^{\hbar}\left(\bar{l}_{ij}\bar{\Xi}_{ij} - \underline{l}_{ij}\underline{\Xi}_{ij}\right) < 0 \tag{21}$$

where

$$\bar{\Upsilon} = \begin{bmatrix} \Lambda_{11} & \Lambda_{12} & \Lambda_{13} \\ * & \Lambda_{22} & 0 \\ * & * & \Lambda_{33} \end{bmatrix}$$

$$\Lambda_{12} = \begin{bmatrix} \bar{\mathcal{P}}_\varrho U_{\alpha\varrho}^T & \sqrt{2}\bar{\mathcal{P}}_\varrho & 0 \\ 0 & 0 & \sqrt{2}\bar{\mathcal{P}}_\varrho \\ 0 & 0 & 0 \end{bmatrix}$$

$$\Lambda_{11} = \begin{bmatrix} \Lambda^1 & \bar{\delta}B_{\alpha\varrho}\bar{\mathcal{W}}_{\ell\varrho} & 0 \\ * & -(1+\theta)\bar{\Psi}_\varrho & 0 \\ * & * & \left(\frac{\theta}{\mu} - \eta\right)I \end{bmatrix}$$

$$\Lambda^1 = A_{\alpha\varrho}\bar{\mathcal{P}}_\varrho + \bar{\mathcal{P}}_\varrho A_{\alpha\varrho}^T + 2\bar{\delta}B_{\alpha\varrho}\bar{\mathcal{W}}_{\ell\varrho} + (1+\theta)\vartheta\bar{\Psi}_\varrho + \epsilon_1^{-1}L_{\alpha\varrho}L_{\alpha\varrho}^T + \epsilon_2\bar{\mathcal{P}}_\varrho$$

$$\Lambda_{22} = -\operatorname{diag}\left\{\epsilon_1^{-1}I, \left(\epsilon_2^{-1}\imath\left(\pi_{\alpha\varrho}^2 + \zeta_\varrho^2 m\left(\bar{\delta}^2 + \tilde{\delta}\right)\right)\right)^{-1} I \right.$$
$$\left. \left(\epsilon_2^{-1}\imath\zeta_\varrho^2 m\left(\bar{\delta}^2 + \tilde{\delta}\right)\right)^{-1} I\right\}$$

$$\Lambda_{13} = \left[\sqrt{\sigma_{\varrho 1}}\bar{\mathcal{P}}_\varrho, \ldots, \sqrt{\sigma_{\varrho c}}\bar{\mathcal{P}}_\varrho\right]$$

$$\Lambda_{33} = -\operatorname{diag}\{\bar{\mathcal{P}}_1, \bar{\mathcal{P}}_2, \ldots, \bar{\mathcal{P}}_c\}.$$

Moreover, the controller gain is given by $\mathcal{W}_{\ell\varrho} = \bar{\mathcal{W}}_{\ell\varrho}\bar{\mathcal{P}}_\varrho^{-1}$.

Proof: Let

$$\bar{\mathcal{P}}_\varrho \triangleq \mathcal{P}_\varrho^{-1}, \bar{\Psi}_\varrho \triangleq \bar{\mathcal{P}}_\varrho^T\Psi_\varrho\bar{\mathcal{P}}_\varrho.$$

By Schur's complement lemma, (10) can be ensured by (20).

Then, by the congruence transformation of (11) with $\operatorname{diag}\{\bar{\mathcal{P}}_\varrho, \bar{\mathcal{P}}_\varrho, I, \ldots, I\}$, one has

$$\sum_{\alpha=1}^{\beta}\sum_{\ell=1}^{\hbar}\varpi_{\alpha\ell}(z(t))\bar{\Upsilon} < 0.$$

Define $\underline{l}_{\alpha\ell}$ and $\bar{l}_{\alpha\ell}$ as global lower and upper bounds on $\nu_{\alpha\ell}(z(t))$, respectively. Suppose that there exist slack matrices $\bar{\Xi}_{\alpha\ell} \geq 0$ and $\underline{\Xi}_{\alpha\ell} \geq 0$ containing upper and lower bound information, respectively, which satisfies the following:

$$\sum_{\alpha=1}^{\beta}\sum_{\ell=1}^{\hbar}(\bar{l}_{\alpha\ell} - \nu_{\alpha\ell}(t))\bar{\Xi}_{\alpha\ell} \geq 0 \tag{22}$$

$$\sum_{\alpha=1}^{\beta}\sum_{\ell=1}^{\hbar}(\nu_{\alpha\ell}(t) - \underline{l}_{\alpha\ell})\underline{\Xi}_{\alpha\ell} \geq 0. \tag{23}$$

Combining (22) and (23), we get

$$\begin{aligned}
&\sum_{\alpha=1}^{\beta}\sum_{\ell=1}^{\hbar}\nu_{\alpha\ell}(t)\bar{\Upsilon} \\
&\leq \sum_{\alpha=1}^{\beta}\sum_{\ell=1}^{\hbar}\nu_{\alpha\ell}(t)\bar{\Upsilon} + \sum_{\alpha=1}^{\beta}\sum_{\ell=1}^{\hbar}(\bar{l}_{\alpha\ell} - \nu_{\alpha\ell}(t))\bar{\Xi}_{\alpha\ell} \\
&\quad + \sum_{\alpha=1}^{\beta}\sum_{\ell=1}^{\hbar}(\nu_{\alpha\ell}(t) - \underline{l}_{\alpha\ell})\underline{\Xi}_{\alpha\ell} \\
&= \sum_{\alpha=1}^{\beta}\sum_{\ell=1}^{\hbar}\nu_{\alpha\ell}(t)(\bar{\Upsilon} - \bar{\Xi}_{\alpha\ell} + \underline{\Xi}_{\alpha\ell}) \\
&\quad + \sum_{i=1}^{\beta}\sum_{j=1}^{\hbar}(\bar{l}_{ij}\bar{\Xi}_{ij} - \underline{l}_{ij}\underline{\Xi}_{ij}) \\
&= \sum_{\alpha=1}^{\beta}\sum_{\ell=1}^{\hbar}\nu_{\alpha\ell}(t)[\bar{\Upsilon} - \bar{\Xi}_{\alpha\ell} + \underline{\Xi}_{\alpha\ell} \\
&\quad + \sum_{i=1}^{\beta}\sum_{j=1}^{\hbar}(\bar{l}_{ij}\bar{\Xi}_{ij} - \underline{l}_{ij}\underline{\Xi}_{ij})].
\end{aligned} \tag{24}$$

Thus, according to (21), one has (11). ■

Remark 9: The general method [15], [16] of dealing with the mismatched membership functions in T-S fuzzy systems is not

suitable for this study. To solve the controller gain, the slack matrices $\bar{\Xi}_{\alpha\ell} \geq 0$ and $\Xi_{\alpha\ell} \geq 0$ are introduced. With the help of upper and lower bounds on $\nu_{\alpha\ell}(t)$, a series of slack conditions is obtained for solvable controller gain, that is, $\bar{\Upsilon} < 0$ is replaced by the condition (21). In fact, if $\bar{\mathcal{P}}_\varrho$, $\bar{\Psi}_\varrho$, and $\bar{\mathcal{W}}_{\ell\varrho}$ are feasible solutions satisfying the conditions (10) and (11), then the variables $\bar{\mathcal{P}}_\varrho$, $\bar{\Psi}_\varrho$, $\bar{\Xi}_{\alpha\ell} = 0$, $\Xi_{\alpha\ell} = 0$, and $\bar{\mathcal{W}}_{\ell\varrho}$ must be feasible solutions for the conditions (20) and (21); otherwise, the feasible solution of the conditions (20) and (21) may not satisfy the conditions (10) and (11). Moreover, compared with the condition (11) in Theorem 1, the condition (21) in Theorem 2 integrates the global boundary information of $\nu_{\alpha\ell}(t)$ with less conservatism.

B. Reachability

The reachability of the sliding region under the designed fuzzy SMC law (8) is discussed.

Theorem 3: Under the fuzzy SMC law (8), the state of system (2) can be driven on the sliding region, and ζ_ϱ satisfies the following:

$$\max_{1\leq\alpha\leq\beta}[\zeta_\varrho\bar{\delta}\|B_{\alpha\varrho}\|]\|\kappa(t)\| - w - \jmath > 0 \tag{25}$$

where $w = \max_{1\leq\alpha\leq\beta}\{\max_{1\leq\ell\leq\hbar}[\bar{\delta}\|\mathcal{R}B_{\alpha\varrho}\mathcal{W}_{\ell\varrho}\|]\}\|\kappa(t)\|$, $\jmath > 0$, and $h_\varrho > 0$ with $h_\varrho = \max_{1\leq\alpha\leq\beta}[\|\mathcal{R}A_{\alpha\varrho}\|] + \max_{1\leq\alpha\leq\beta}[\|\mathcal{R}L_{\alpha\varrho}\|\|U_{\alpha\varrho}\|] + \max_{1\leq\alpha\leq\beta}\{\max_{1\leq\ell\leq\hbar}[\bar{\delta}\|\mathcal{R}B_{\alpha\varrho}\mathcal{W}_{\ell\varrho}\|]\} + \max_{1\leq\alpha\leq\beta}[\pi_{\alpha\varrho}\|\mathcal{R}B_{\alpha\varrho}\|] - \max_{1\leq\alpha\leq\beta}[\zeta_\varrho\bar{\delta}\|B_{\alpha\varrho}\|]$.

Proof: Construct the Lyapunov function

$$\mathcal{V}_2(\gamma(t)) = \frac{1}{2}\gamma^T(t)\gamma(t). \tag{26}$$

Then, one has

$$\begin{aligned}
&\mathbb{E}\{\Im\mathcal{V}_2(\gamma(t))\} = \mathbb{E}\{\gamma^T(t)\dot{\gamma}(t)\} \\
&= \mathbb{E}\Bigg\{\gamma^T(t)\sum_{\alpha=1}^{\beta}\sum_{\ell=1}^{\hbar}\nu_{\alpha\ell}(z(t))\mathcal{R}[(A_{\alpha\varrho} + \triangle A_{\alpha\varrho}(t) \\
&\quad + \delta(t_s)B_{\alpha\varrho}\mathcal{W}_{\ell\varrho})z(t) + \delta(t_s)B_{\alpha\varrho}\mathcal{W}_{\ell\varrho}\kappa(t) \\
&\quad + B_{\alpha\varrho}(\varphi_{\alpha\varrho}(z(t),t) - \zeta_\varrho\|\check{z}(t_s)\|\text{sign}(\gamma(t)))]\Bigg\} \\
&\leq \|\gamma(t)\|\Bigg\{\Bigg[\max_{1\leq\alpha\leq\beta}[\|\mathcal{R}A_{\alpha\varrho}\|] + \max_{1\leq\alpha\leq\beta}[\|\mathcal{R}L_{\alpha\varrho}\|\|U_{\alpha\varrho}\|] \\
&\quad + \max_{1\leq\alpha\leq\beta}\left\{\max_{1\leq\ell\leq\hbar}[\bar{\delta}\|\mathcal{R}B_{\alpha\varrho}\mathcal{W}_{\ell\varrho}\|]\right\} \\
&\quad + \max_{1\leq\alpha\leq\beta}[\pi_{\alpha\varrho}\|\mathcal{R}B_{\alpha\varrho}\|]\Bigg]\|z(t)\| \\
&\quad + \max_{1\leq\alpha\leq\beta}\left\{\max_{1\leq\ell\leq\hbar}[\bar{\delta}\|\mathcal{R}B_{\alpha\varrho}\mathcal{W}_{\ell\varrho}\|]\right\}\|\kappa(t)\|\Bigg\} \\
&\quad - \max_{1\leq\alpha\leq\beta}[\zeta_\varrho\bar{\delta}\|B_{\alpha\varrho}\|]\|z(t_s)\|\|\gamma(t)\| \\
&\leq \|\gamma(t)\|\left[h_\varrho\|z(t)\| - \left(\max_{1\leq\alpha\leq\beta}[\zeta_\varrho\bar{\delta}\|B_{\alpha\varrho}\|]\|\kappa(t)\| - w - \jmath\right)\right] \\
&\quad - \jmath\|\gamma(t)\|
\end{aligned} \tag{27}$$

where $w = \max_{1\leq\alpha\leq\beta}\{\max_{1\leq\ell\leq\hbar}[\bar{\delta}\|\mathcal{R}B_{\alpha\varrho}\mathcal{W}_{\ell\varrho}\|]\}\|\kappa(t)\|$ and $h_\varrho = \max_{1\leq\alpha\leq\beta}[\|\mathcal{R}A_{\alpha\varrho}\|] + \max_{1\leq\alpha\leq\beta}[\|\mathcal{R}L_{\alpha\varrho}\|\|U_{\alpha\varrho}\|] + \max_{1\leq\alpha\leq\beta}\{\max_{1\leq\ell\leq\hbar}[\bar{\delta}\|\mathcal{R}B_{\alpha\varrho}\mathcal{W}_{\ell\varrho}\|]\} + \max_{1\leq\alpha\leq\beta}[\pi_{\alpha\varrho}\|\mathcal{R}B_{\alpha\varrho}\|] - \max_{1\leq\alpha\leq\beta}[\zeta_\varrho\bar{\delta}\|B_{\alpha\varrho}\|]$.

Defining the sliding region

$$\Theta \triangleq \left\{z(t) : h_\varrho\|z(t)\| \leq \max_{1\leq\alpha\leq\beta}[\zeta_\varrho\bar{\delta}\|B_{\alpha\varrho}\|]\|z(t)\| - w - \jmath\right\}.$$

Then, we can get

$$\mathbb{E}\{\Im\mathcal{V}_2(\gamma(t))\} \leq -\jmath\|\gamma(t)\| = -\jmath\sqrt{2\mathcal{V}_2(\gamma(t))}. \tag{28}$$

For $t \geq \bar{T}$, there exists an instant $\bar{T} \leq \sqrt{2\mathcal{V}_2(0)}/\jmath = \|\mathcal{R}z(0)\|/\jmath$, such that $\mathcal{V}_2(\gamma(t)) = 0$, that is $\gamma(t) = 0$.

Therefore, the reachability of the sliding region is achieved. ■

Remark 10: Due to the existence of sign function, the chattering phenomenon will inevitably occur during the sliding motion, and the trajectory cannot be guaranteed to stay on the sliding surface all the time. In this case, we find a reasonable sliding region Θ, where the sliding motion can always remain in a bounded neighborhood near the predefined sliding surface.

C. Zeno-Free Analysis

The dynamic ETP can effectively reduce the unnecessary data transmission. But for continuous-time systems, to avoid Zeno behavior is essential. In the following, a lower bound on the triggered interval is given to avoid Zeno behavior.

Theorem 4: For system (2), the dynamic ETP condition (3) can ensure that the triggered interval $t_{s+1} - t_s$ is satisfied

$$t_{s+1} - t_s \geq \frac{1}{r}\ln\left[1 + \frac{r(\iota(t_{s+1}) + \mu\vartheta z^T(t_{s+1})\Psi_\varrho z(t_{s+1}))}{j\mu\lambda_{\max}(\Psi_\varrho)}\right] \tag{29}$$

where $r = \|\tilde{\mathcal{A}}\| + \|\tilde{\mathcal{L}}\|\|\tilde{\mathcal{U}}\| + \tilde{\pi}\|\tilde{\mathcal{B}}\| + \|\tilde{\mathcal{B}}\tilde{\mathcal{W}}\| - \zeta_\varrho\|\tilde{\mathcal{B}}\|\|\check{z}(t_s)\|$, $j = [\|\tilde{\mathcal{A}}\| + \|\tilde{\mathcal{L}}\|\|\tilde{\mathcal{U}}\| + \tilde{\pi}\|\tilde{\mathcal{B}}\|]\|z(t)\|^2 + \|\tilde{\mathcal{B}}\tilde{\mathcal{W}}\|\|\check{z}(t_s)\|^2 - \zeta_\varrho m\|\tilde{\mathcal{B}}\|\|\check{z}(t_s)\|$ with $\tilde{\mathcal{A}} = \sum_{\alpha=1}^{\beta}\sum_{\ell=1}^{\hbar}\nu_{\alpha\ell}(z(t))A_{\alpha\varrho}$, $\tilde{\mathcal{B}} = \sum_{\alpha=1}^{\beta}\sum_{\ell=1}^{\hbar}\nu_{\alpha\ell}(z(t))B_{\alpha\varrho}$, $\tilde{\mathcal{L}} = \sum_{\alpha=1}^{\beta}\sum_{\ell=1}^{\hbar}\nu_{\alpha\ell}(z(t))L_{\alpha\varrho}$, $\tilde{\mathcal{U}} = \sum_{\alpha=1}^{\beta}\sum_{\ell=1}^{\hbar}\nu_{\alpha\ell}(z(t))U_{\alpha\varrho}$, $\tilde{\mathcal{W}} = \sum_{\alpha=1}^{\beta}\sum_{\ell=1}^{\hbar}\nu_{\alpha\ell}(z(t))W_{\ell\varrho}$, and $\tilde{\pi} = \sum_{\alpha=1}^{\beta}\sum_{\ell=1}^{\hbar}\nu_{\alpha\ell}(z(t))\pi_{\alpha\varrho}$.

Proof: For the error $\kappa(t) = z(t_s) - z(t)$, one can obtain

$$\begin{aligned}
\dot{\kappa}(t) = &-\sum_{\alpha=1}^{\beta}\sum_{\ell=1}^{\hbar}\nu_{\alpha\ell}(z(t))[(A_{\alpha\varrho} + \triangle A_{\alpha\varrho}(t))z(t) \\
&+ B_{\alpha\varrho}\mathcal{W}_{\ell\varrho}\check{z}(t_s) + B_{\alpha\varrho}(\varphi_{\alpha\varrho}(z(t),t) \\
&- \zeta_\varrho\|\check{z}(t_s)\|\text{sign}(\gamma(t)))].
\end{aligned} \tag{30}$$

When $\forall t \in [t_s, t_{s+1})$, one has

$$\begin{aligned}
&\frac{d}{dt}\|\kappa(t)\|^2 \leq 2\|\kappa(t)\|\|\dot{\kappa}(t)\| \\
&\leq [\|\tilde{\mathcal{A}}\| + \|\tilde{\mathcal{L}}\|\|\tilde{\mathcal{U}}\| + \tilde{\pi}\|\tilde{\mathcal{B}}\|](\|z(t)\|^2 + \|\kappa(t)\|^2) \\
&\quad + \|\tilde{\mathcal{B}}\tilde{\mathcal{W}}\|(\|\check{z}(t_s)\|^2 + \|\kappa(t)\|^2) \\
&\quad - \zeta_\varrho\|\tilde{\mathcal{B}}\|\|\check{z}(t_s)\|(m + \|\kappa(t)\|^2)
\end{aligned}$$

$$= [\|\tilde{\mathcal{A}}\| + \|\tilde{\mathcal{L}}\|\|\tilde{\mathcal{U}}\| + \tilde{\pi}\|\tilde{\mathcal{B}}\| - \zeta_\varrho\|\tilde{\mathcal{B}}\|\|\breve{z}(t_s)\| + \|\tilde{\mathcal{B}}\tilde{\mathcal{W}}\|]\|\kappa(t)\|^2 + [\|\tilde{\mathcal{A}}\| + \|\tilde{\mathcal{L}}\|\|\tilde{\mathcal{U}}\| + \tilde{\pi}\|\tilde{\mathcal{B}}\|]\|z(t)\|^2 + \|\tilde{\mathcal{B}}\tilde{\mathcal{W}}\|\|\breve{z}(t_s)\|^2 - \zeta_\varrho m\|\tilde{\mathcal{B}}\|\|\breve{z}(t_s)\|$$
$$\triangleq r\|\kappa(t)\|^2 + j. \tag{31}$$

With the help of comparison Lemma, at the triggered time $e(t_s) = 0$, it can be got that

$$\|\kappa(t_{s+1})\|^2 \leq \frac{r}{j}\left(e^{r(t_{s+1}-t_s)} - 1\right). \tag{32}$$

Combining with the dynamic ETP condition (3), we can get

$$\frac{\iota(t_{s+1}) + \mu\vartheta z^T(t_{s+1})\Psi_\varrho z(t_{s+1})}{\mu\lambda_{\max}(\Psi_\varrho)} \leq \|\kappa(t_{s+1})\|^2. \tag{33}$$

From (32) and (33), the triggered interval is obtained that

$$t_{s+1} - t_s \geq \frac{1}{r}\ln\left[1 + \frac{r(\iota(t_{s+1}) + \mu\vartheta z^T(t_{s+1})\Psi_\varrho z(t_{s+1}))}{j\mu\lambda_{\max}(\Psi_\varrho)}\right] \triangleq T^\star. \tag{34}$$

Due to $\mu > 0$, one has

$$r(\iota(t_{s+1}) + \mu\vartheta z^T(t_{s+1})\Psi_\varrho z(t_{s+1})) > 0.$$

Therefore, we can find a lower bound $T^\star > 0$ to avoid the Zeno phenomenon. ■

Remark 11: In order to realize the practical application of ETP, it is required that the triggered time generated by the ETP should not be too dense, otherwise it cannot be realized in practice. That is to make sure that the ETP avoids the Zeno phenomenon. A general approach is to find a lower bound about the event-triggered interval. Based on this, Theorem 4 combines the dynamic ETP condition (3) and proves the lower bound $T^\star$ of two adjacent trigger intervals, which can effectively avoid Zeno behavior.

IV. Case Study

Consider the tunnel diode circuit model [28], expressed as

$$\begin{aligned}\mathcal{H}_1\dot{z}_1(t) &= -\tilde{\mu}z_1(t) - \tilde{\xi}_\varrho z_1^2(t) + z_2(t)\\ \mathcal{H}_2\dot{z}_2(t) &= -z_1(t) - \mathcal{H}_3 z_2(t) + u(t) + \varphi(t)\end{aligned} \tag{35}$$

where $z(t) = [z_1^T(t)\, z_2^T(t)]^T$ denotes the deviation variables. The values of parameters $\mathcal{H}_1$, $\mathcal{H}_2$, and $\mathcal{H}_3$ are given as 20 mF, 1000 mH, and 10 Ω, respectively. Define $\tilde{\mu} = 0.002 + \Delta\tilde{\mu}z_1^2(t)$ with $\Delta\tilde{\mu} \in [0.01, 0.03]$.

Consider two fuzzy rules $\alpha = 1, 2$, $\ell = 1, 2$, and the parameter $\tilde{\xi}_\varrho$ obeys SMP with two switching modes: $\tilde{\xi}_1 = 0.01$ and $\tilde{\xi}_2 = 0.02$. The IT2F model is adopted to represent the uncertain information. Supposing $\|z_1(t)\| \leq 3$, one has $\tilde{\mu}_{\max} = 0.272$ and $\tilde{\mu}_{\min} = 0.002$. Then, the system model with upper and lower membership functions can be obtained as

$$\dot{z}(t) = \sum_{\alpha=1}^{2}\varpi_\alpha(z(t))[(A_{\alpha\varrho} + \triangle A_{\alpha\varrho}(t))z(t) + B_{\alpha\varrho}(u(t) + \varphi_{\alpha\varrho}(z(t), t))] \tag{36}$$

where

$$A_{11} = \begin{bmatrix}\frac{-\tilde{\mu}_{\min}}{\mathcal{H}_1} & 50\\ -1 & -10\end{bmatrix}, A_{12} = \begin{bmatrix}\frac{-\tilde{\mu}_{\max}}{\mathcal{H}_1} & 50\\ -1 & -10\end{bmatrix}$$
$$A_{21} = \begin{bmatrix}-4.6 & 50\\ -1 & -10\end{bmatrix}, A_{22} = \begin{bmatrix}-22.6 & 50\\ -1 & -10\end{bmatrix}$$
$$B_{11} = B_{12} = \begin{bmatrix}0 & 1\end{bmatrix}^T, B_{21} = \begin{bmatrix}0 & 1.1\end{bmatrix}^T$$
$$B_{22} = \begin{bmatrix}0 & 0.9\end{bmatrix}^T, \varphi_{\alpha\varrho}(z(t), t) = 0.5z_1^2\cos(t)$$
$$\underline{\varpi}_1(z_1(t)) = \frac{\tilde{\mu}_{\max} - \tilde{\mu}_1(t)}{\tilde{\mu}_{\max} - \tilde{\mu}_{\min}}, \bar{\varpi}_1(z_1(t)) = \frac{\tilde{\mu}_{\max} - \tilde{\mu}_2(t)}{\tilde{\mu}_{\max} - \tilde{\mu}_{\min}}$$
$$\underline{\varpi}_2(z_1(t)) = \frac{\tilde{\mu}_2(t) - \tilde{\mu}_{\min}}{\tilde{\mu}_{\max} - \tilde{\mu}_{\min}}, \bar{\varpi}_2(z_1(t)) = \frac{\tilde{\mu}_1(t) - \tilde{\mu}_{\min}}{\tilde{\mu}_{\max} - \tilde{\mu}_{\min}}$$
$$\tilde{\mu}_1(t) = 0.002 + 0.003z_1^2(t), \tilde{\mu}_2(t) = 0.002 + 0.001z_1^2(t)$$
$$\underline{\phi}_\alpha(z(t)) = \sin^2(z_1(t)), \bar{\phi}_\alpha(z(t)) = 1 - \sin^2(z_1(t))$$

and $\triangle A_{\alpha\varrho}(t) = L_{\alpha\varrho}E_{\alpha\varrho}(t)U_{\alpha\varrho}$ is the parameter uncertainty with $L_{11} = [0.95; 0.1]$, $L_{12} = [1; 0.2]$, $L_{21} = [1.2; 0.3]$, $L_{22} = [1.1; 0.2]$, $U_{11} = [0.95; 0.1]^T$, $U_{12} = [1; 0.2]^T$, $U_{21} = [1.1; 0.3]^T$, and $U_{22} = [0.9; 0.2]^T$.

Consider the membership functions as: $\nu_1(\breve{z}_1(t)) = \underline{\varpi}_1(\breve{z}_1(t))\underline{\psi}_1(\breve{z}_1(t)) + \bar{\varpi}_1(\breve{z}_1(t))\bar{\psi}_1(\breve{z}_1(t))$, and $\nu_2(\breve{z}_1(t)) = 1 - \nu_1(\breve{z}_1(t))$ with $\underline{\psi}_1(\breve{z}_1(t)) = 0.5$. In addition, the parameters $\underline{l}_{\alpha\ell}$ and $\bar{l}_{\alpha\ell}$ are set as $\underline{l}_{11} = 0.1951$, $\underline{l}_{12} = 0.2096$, $\underline{l}_{21} = 0.1418$, $\underline{l}_{22} = 0.1523$, $\bar{l}_{11} = 0.3675$, $\bar{l}_{12} = 0.3870$, $\bar{l}_{21} = 0.2925$, and $\bar{l}_{22} = 0.3080$, respectively.

The TR matrix is chosen as

$$\Sigma(\tau) = \begin{bmatrix}-0.5\tau & 0.5\tau\\ 3\tau^2 & -3\tau^2\end{bmatrix}.$$

Assume that the ST follows the Weibull distribution with probability distribution function $\omega_1(\tau) = 0.5\tau e^{-0.25\tau^2}$ and $\omega_2(\tau) = 3\tau^2 e^{-\tau^3}$. Then, according to $\mathbb{E}[\sigma_{\varrho\varsigma}(\tau)] = \int_0^\infty \sigma_{\varrho\varsigma}(\tau)\omega_\varrho(\tau)d\tau$, one has the following:

$$\mathbb{E}\{\Sigma(\tau)\} = \begin{bmatrix}-0.8862 & 0.8862\\ 2.7082 & -2.7082\end{bmatrix}.$$

Choose the fading parameters $\bar{\delta} = 0.8$, $\tilde{\delta} = 0.05$, $\mathcal{R} = [1\,1]$, $\pi_{\alpha\varrho} = 0.2$, $\mu = 0.6$, $\vartheta = 0.2$, $\theta = 0.1$, $\eta = 0.1$, $\iota = 0.2$, and $\jmath = 0.2$. According to Theorem 2, we get

$$\mathcal{W}_{11} = \begin{bmatrix}0.2964 & 4.3574\end{bmatrix}, \mathcal{W}_{12} = \begin{bmatrix}-0.0269 & 4.3712\end{bmatrix}$$
$$\mathcal{W}_{21} = \begin{bmatrix}0.1164 & 4.0217\end{bmatrix}, \mathcal{W}_{22} = \begin{bmatrix}-0.1250 & 4.8557\end{bmatrix}.$$

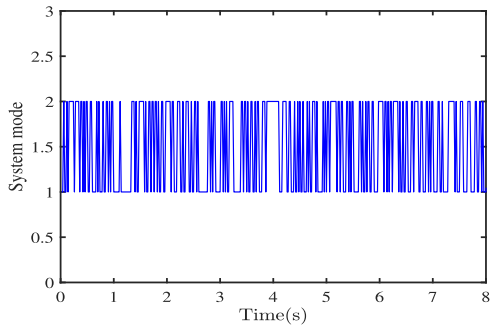

Fig. 2. System mode.

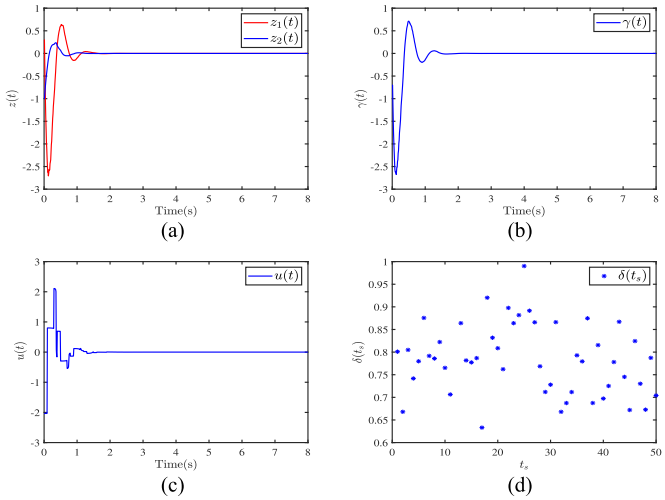

Fig. 3. (a) System response $z(t)$, (b) sliding function $\gamma(t)$, and (c) control input $u(t)$ with $\bar{\delta} = 0.8$. Fading coefficient $\bar{\delta}(t_s)$.

TABLE I
TRIGGERING NUMBER UNDER DIFFERENT FADING CHANNELS

Fading channel	$\delta = 0.8$	$\delta = 0.5$	$\delta = 0.2$
Triggering number	53	71	89

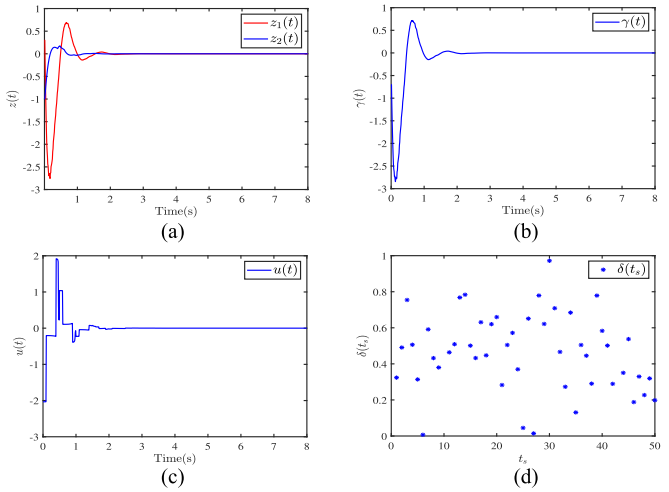

Fig. 4. (a) System response $z(t)$, (b) sliding function $\gamma(t)$, and (c) control input $u(t)$ with $\bar{\delta} = 0.5$. Fading coefficient $\bar{\delta}(t_s)$.

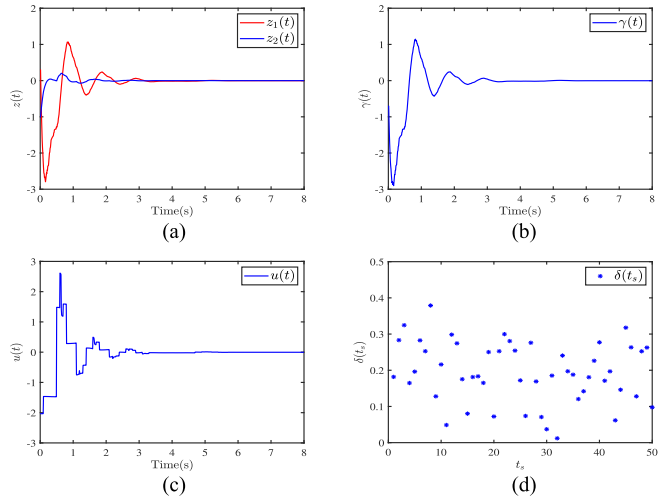

Fig. 5. (a) System response $z(t)$, (b) sliding function $\gamma(t)$, and (c) control input $u(t)$ with $\bar{\delta} = 0.2$. Fading coefficient $\bar{\delta}(t_s)$.

For given $z(0) = [0.3 - 1.0]^T$ and $\iota(0) = 0.3$, Fig. 2 shows the system mode and the mode switching of S-MJSs. The trajectory of system state $z(t)$ is shown in Fig. 3(a). Fig. 3(b) and (c) shows the sliding function $\gamma(t)$ and the input signal $u(t)$. Obviously, under the designed fuzzy sliding mode controller, the system state tends to zero, indicating that the tunnel diode circuit system has achieved the stochastic stability. Moreover, Fig. 3(d) stands for the fading coefficient $\delta(t_s)$, reflecting the random decay degree. Fig. 7(a) and (b) represents the release intervals and the dynamic variable $\iota(t)$ of dynamic ETP.

According to the fading model (5), the parameter $\delta \in [0, 1]$ is a random variable with the mathematical expectation $\bar{\delta}$. In order to better reflect the performance of the model under different transmission conditions, this work simulates three different fading channels, that is, $\bar{\delta} = 0.8$, $\bar{\delta} = 0.5$, and $\bar{\delta} = 0.2$. The triggered number is given in Table I, and the simulation results are shown in Figs. 3–5. According to the trajectory of system response $z(t)$, sliding function $\gamma(t)$, and control input $u(t)$, it can be seen that the smaller the value of $\bar{\delta}$, the more prone the transmission channel is to fading phenomenon, the slower the system convergence rate, and the worse the performance. As a result of fading phenomenon, the transmitted signals cannot accurately reach the controller, and even cause data packet loss in serious cases. According to Table I, the system will trigger and transmit more signals to compensate for the lack of performance.

Moreover, in order to reflect the advantage of dynamic ETP, the static ETP is simulated under the same parameters. Fig. 6(d) shows the release intervals under the static ETP [9]. Compared with Figs. 7(a) and 6(d), the number of signals triggered and transmitted under the dynamic ETP is less than that under the static ETP, which means that the dynamic ETP can reduce network load more than the static ETP. Next, we compare the

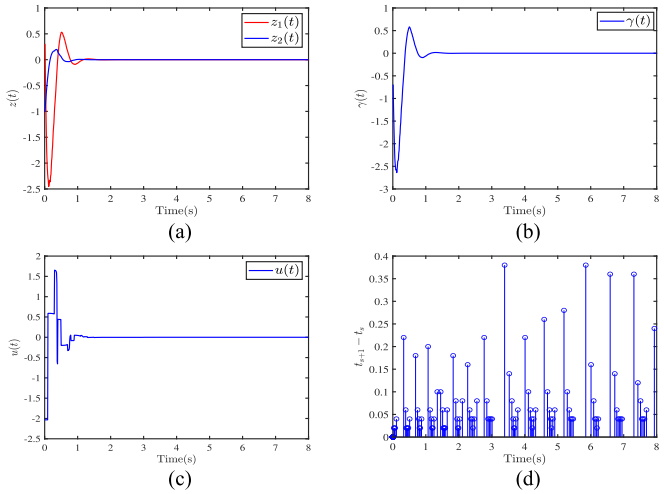

Fig. 6. (a) System response $z(t)$, (b) sliding function $\gamma(t)$, and (c) control input $u(t)$ under the static ETP [9]. (d) Release intervals.

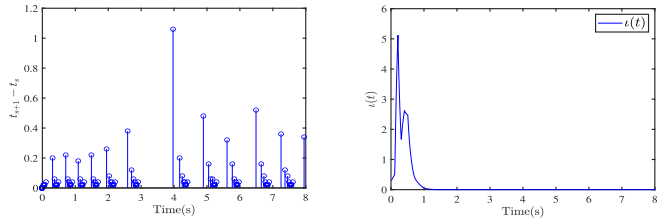

Fig. 7. Release instants and variable $\iota(t)$ under the dynamic ETP. (a) Release intervals. (b) Dynamic variable $\iota(t)$.

performance of the controller and the convergence speed of system states. According to the trajectory of system response $z(t)$, slide function $\gamma(t)$, and control input $u(t)$ in Figs. 3 and 6, it can be seen that the two ETPs can achieve similar control performance. It is further shown that the dynamic ETP can save network resources more effectively than the static ETP.

V. Conclusion

The SMC problem has been studied for IT2F S-MJSs with channel fading. Signals triggered by the dynamic ETP are subject to unpredictable channel fading before reaching the controller. Based on a common sliding mode surface, a fuzzy sliding mode controller has been constructed to be affected by the dynamic ETP and the fading signal. The boundary information of the global membership function has been adopted to deal with the mismatched membership functions, and sufficient criteria have been proposed to ensure the stochastic stability and the accessibility of the sliding dynamics. Finally, the effectiveness of the proposed method is proved by a practical circuit model. However, the research results in this work are based on the condition of modal synchronization between the system and the controller, which brings some conservative results. In future work, the asynchronous SMC problem for IT2F S-MJSs with channel fading will be investigated.

References

[1] E. Boukas, *Stochastic Switching Systems: Analysis and Design*. Berlin, Germany: Birkhäuser, 2005.
[2] S. L. Dong, C. L. P. Chen, M. Fang, and Z. G. Wu, "Dissipativity-based asynchronous fuzzy sliding mode control for T-S fuzzy hidden Markov jump systems," *IEEE Trans. Cybern.*, vol. 50, no. 9, pp. 4020–4030, Sep. 2020.
[3] M. Xue, H. C. Yan, H. Zhang, J. Sun, and H. K. Lam, "Hidden-Markov-model-based asynchronous H_∞ tracking control of fuzzy Markov jump systems," *IEEE Trans. Fuzzy Syst.*, vol. 29, no. 5, pp. 1081–1092, May 2021.
[4] S. Kuppusamy, Y. H. Joo, and H. S. Kim, "Asynchronous control for discrete-time hidden Markov jump power systems," *IEEE Trans. Cybern.*, vol. 52, no. 9, pp. 9943–9948, Sep. 2022.
[5] G. T. Ran, C. J. Li, R. Sakthivel, C. S. Han, B. H. Wang, and J. Liu, "Adaptive event-triggered asynchronous control for interval type-2 fuzzy Markov jump systems with cyberattacks," *IEEE Trans. Fuzzy Syst.*, vol. 9, no. 1, pp. 88–99, Mar. 2022.
[6] T. Fjeldstad and H. Omre, "Bayesian inversion of convolved hidden Markov models with applications in reservoir prediction," *IEEE Trans. Geosci. Remote Sens.*, vol. 58, no. 3, pp. 1957–1968, Mar. 2020.
[7] X. W. Mu and Z. H. Hu, "Impulsive consensus of stochastic multi-agent systems under semi-Markovian switching topologies and application," *Automatica*, vol. 150, Apr. 2022, Art. no. 110871.
[8] Y. X. Tian, H. C. Yan, H. Zhang, X. S. Zhan, and Y. Peng, "Resilient static output feedback control of linear semi-Markov jump systems with incomplete semi-Markov kernel," *IEEE Trans. Autom. Control*, vol. 66, no. 9, pp. 4274–4281, Sep. 2021.
[9] J. Wang, T. T. Ru, H. Shen, and V. Sreeram, "Asynchronous event-triggered sliding mode control for semi-Markov jump systems within a finite-time interval," *IEEE Trans. Circuits Syst. I., Regular Papers*, vol. 68, no. 1, pp. 458–468, Jan. 2021.
[10] H. Shen, M. P. Xing, S. Y. Xu, M. V. Basin, and J. H. Park, "H_∞ stabilization of discrete-time nonlinear semi-Markov jump singularly perturbed systems with partially known semi-Markov kernel information," *IEEE Trans. Circuits Syst. I., Regular Papers*, vol. 68, no. 2, pp. 818–828, Feb. 2021.
[11] Z. P. Ning, B. Cai, R. Weng, L. X. Zhang, and S. F. Su, "Stability and control of fuzzy semi-Markov jump systems under unknown semi-Markov kernel," *IEEE Trans. Fuzzy Syst.*, vol. 30, no. 7, pp. 2452–2465, Jul. 2022.
[12] X. T. Wu, P. Shi, Y. Tang, S. Mao, and F. Qian, "Stability analysis of semi-Markov jump stochastic nonlinear systems," *IEEE Trans. Autom. Control*, vol. 67, no. 4, pp. 2084–2091, Apr. 2022.
[13] L. C. Zhang, Y. H. Sun, H. K. Lam, H. Y. Li, J. X. Wang, and D. C. Hou, "Guaranteed cost control for interval type-2 fuzzy semi-Markov switching systems within a finite-time interval," *IEEE Trans. Fuzzy Syst.*, vol. 30, no. 7, pp. 2583–2594, Jul. 2022.
[14] X. W. Mu and Z. H. Hu, "Stability analysis for semi-Markovian switched singular stochastic systems," *Automatica*, vol. 118, Aug. 2022, Art. no. 109014.
[15] A. Sala and C. Arino, "Relaxed stability and performance conditions for Takagi-Sugeno fuzzy systems with knowledge on membership function overlap," *IEEE Trans. Syst. Man, Cybern.*, vol. 37, no. 3, pp. 727–732, Jun. 2007.
[16] D. W. Zhang, Q. L. Han, and X. C. Jia, "Network-based output tracking control for a class of T-S fuzzy systems that can not be stabilized by nondelayed output feedback controllers," *IEEE Trans. Cybern.*, vol. 45, no. 8, pp. 1511–1524, Aug. 2015.
[17] J. Wang, C. Y. Yang, J. W. Xia, Z. G. Wu, and H. Shen, "Observer-based sliding mode control for networked fuzzy singularly perturbed systems under weighted try-once-discard protocol," *IEEE Trans. Fuzzy Syst.*, vol. 30, no. 6, pp. 1889–1899, Jun. 2022.
[18] N. N. Karnik, J. M. Mendel, and Q. L. Liang, "Type-2 fuzzy logic systems," *IEEE Trans. Fuzzy Syst.*, vol. 7, no. 6, pp. 643–658, Dec. 1999.
[19] H. G. Han, Z. Liu, H. X. Liu, J. F. Qiao, and C. L. P. Chen, "Type-2 fuzzy broad learning system," *IEEE Trans. Cybern.*, vol. 52, no. 10, pp. 10352–10363, Oct. 2022.
[20] H. K. Lam and L. D. Seneviratne, "Stability analysis of interval type-2 fuzzy-model-based control systems," *IEEE Trans. Syst., Man, Cybern. B, Cybern.*, vol. 38, no. 3, pp. 617–628, Oct. 2008.
[21] H. K. Lam, "A review on stability analysis of continuous-time fuzzy-model-based control systems: From membership-function-independent to membership-function-dependent analysis," *Eng. Appl. Artif. Intel.*, vol. 67, pp. 390–408, Jan. 2018.

[22] Y. K. Yang, Y. G. Niu, and Z. N. Zhang, "Dynamic event-triggered sliding mode control for interval type-2 fuzzy systems with fading channels," *ISA Trans.*, vol. 110, pp. 53–62, Apr. 2021.
[23] Z. N. Zhang, S. F. Su, and Y. G. Niu, "Dynamic event-triggered control for interval type-2 fuzzy systems under fading channel," *IEEE Trans. Cybern.*, vol. 51, no. 11, pp. 5342–5351, Nov. 2021.
[24] A. Al-Mahturi, F. Santoso, M. A. Garratt, and S. G. Anavatti, "A robust self-adaptive interval type-2 TS fuzzy logic for controlling multi-input-multi-output nonlinear uncertain dynamical systems," *IEEE Trans. Syst., Man, Cybern., Syst.*, vol. 52, no. 1, pp. 655–666, Jan. 2022.
[25] L. C. Zhang, H. K. Lam, Y. H. Sun, and H. J. Liang, "Fault detection for fuzzy semi-Markov jump systems based on interval type-2 fuzzy approach," *IEEE Trans. Fuzzy Syst.*, vol. 28, no. 10, pp. 2375–2388, Oct. 2020.
[26] X. Zhang et al., "Asynchronous fault detection for interval type-2 fuzzy nonhomogeneous higher-level Markov jump systems with uncertain transition probabilities," *IEEE Trans. Fuzzy Syst.*, vol. 30, no. 7, pp. 2487–2499, Jul. 2022.
[27] H. Dong and S. S. Zhou, "Extended dissipativity and dynamical output feedback control for interval type-2 singular semi-Markovian jump fuzzy systems," *Int. J. Syst. Sci.*, vol. 53, no. 9, pp. 1906–1924, Jul. 2022.
[28] J. Liu, G. T. Ran, Y. Q. Huang, C. S. Han, Y. Yu, and C. Y. Sun, "Adaptive event-triggered finite-time dissipative filtering for interval type-2 fuzzy Markov jump systems with asynchronous modes," *IEEE Trans. Cybern.*, vol. 52, no. 9, pp. 9709–9721, Sep. 2022.
[29] J. Xu, Y. G. Niu, C. C. Lim, and P. Shi, "Memory output-feedback integral sliding mode control for Furuta pendulum systems," *IEEE Trans. Circuits Syst. I., Reg. Papers*, vol. 67, no. 6, pp. 2042–2052, Jun. 2020.
[30] E. Moulay, V. Lechappe, E. Bernuau, M. Defoort, and F. Plestan, "Fixed-time sliding mode control with mismatched disturbances," *Automatica*, vol. 136, Feb. 2022, Art. no. 110009.
[31] M. Van and S. S. Ge, "Adaptive fuzzy integral sliding-mode control for robust fault-tolerant control of robot manipulators with disturbance observer," *IEEE Trans. Fuzzy Syst.*, vol. 29, no. 5, pp. 1284–1296, May 2021.
[32] Z. Echreshavi, M. Farbood, and M. Shasadeghi, "Fuzzy event-triggered integral sliding mode control of nonlinear continuous-time systems," *IEEE Trans. Fuzzy Syst.*, vol. 30, no. 7, pp. 2347–2359, Jul. 2022.
[33] F. B. Li, C. L. Du, C. H. Yang, L. G. Wu, and W. H. Gui, "Finite-time asynchronous sliding mode control for Markovian jump systems," *Automatica*, vol. 109, Nov. 2019, Art. no. 108503.
[34] Z. R. Cao, Y. G. Niu, and J. Song, "Finite-time sliding-mode control of Markovian jump cyber-physical systems against randomly occurring injection attacks," *IEEE Trans. Autom. Control*, vol. 65, no. 3, pp. 1264–1271, Mar. 2020.
[35] W. H. Qi, G. D. Zong, Y. K. Hou, and M. Chadli, "SMC for discrete-time nonlinear semi-Markovian switching systems with partly unknown semi-Markov kernel," *IEEE Trans. Autom. Control*, vol. 68, no. 3, pp. 1855–1861, Mar. 2023, doi: 10.1109/TAC.2022.3169584.
[36] R. Nie, S.p. He, F. Liu, and X.L. Luan, "Sliding mode controller design for conic-type nonlinear semi-Markovian jumping systems of time-delayed chua's circuit," *IEEE Trans. Syst., Man, Cybern., Syst.*, vol. 51, no. 4, pp. 2467–2475, Apr. 2022.
[37] B. P. Jiang and C. C. Gao, "Decentralized adaptive sliding mode control of large-scale semi-Markovian jump interconnected systems with dead-zone input," *IEEE Trans. Autom. Control*, vol. 67, no. 3, pp. 1521–1528, Mar. 2022.
[38] J. Song, Z. D. Wang, Y. G. Niu, and H. L. Dong, "Genetic-algorithm-assisted sliding-mode control for networked state-saturated systems over hidden Markov fading channels," *IEEE Trans. Cybern.*, vol. 51, no. 7, pp. 3664–3675, Jul. 2021.
[39] Y. N. Shan, K. She, S. M. Zhong, J. Cheng, W. Y. Wang, and C. Zhao, "Event-triggered passive control for Markovian jump discrete-time systems with incomplete transition probability and unreliable channels," *J. Franklin I.*, vol. 356, no. 15, pp. 8093–8117, Oct. 2019.
[40] Y. Liu, A. Tang, and X. D. Wang, "Joint scheduling and power optimization for delay constrained transmissions in coded caching over wireless fading channels," *IEEE Trans. Wireless Commun.*, vol. 21, no. 3, pp. 2093–2106, Mar. 2022.
[41] Y. Yan, R. Wang, S. H. Yu, C. L. Wang, and T. S. Li, "Event-triggered output feedback sliding mode control of mechanical systems," *Nonlinear Dyn.*, vol. 107, no. 4, pp. 3543–3555, Mar. 2022.
[42] X. X. Liu, X. J. Su, P. Shi, C. Shen, and Y. Peng, "Event-triggered sliding mode control of nonlinear dynamic systems," *Automatica*, vol. 112, Feb. 2020, Art. no. 108738.
[43] B. Chen, Y. Y. Zou, and Y. G. Niu, "Dynamic event-triggered sliding mode security control for Markovian jump systems: Learning-based iteration optimization method," *Int. J. Robust Nonlinear Control*, vol. 32, no. 5, pp. 2500–2517, Mar. 2022.
[44] K. Yiu and D. D. Yang, "Output feedback L_1 control of positive Markov jump systems: A dynamic event-triggered method," *J. Franklin I.*, vol. 359, no. 8, pp. 3631–3655, May 2022.
[45] K. Liu and Z. J. Ji, "Dynamic event-triggered consensus of general linear multi-agent systems with adaptive strategy," *IEEE Trans. Circuits Syst. II, Exp. Briefs*, vol. 69, no. 8, pp. 3440–3444, Aug. 2022.

Wenhai Qi (Senior Member, IEEE) received the B.S. degree in automation and the M.S. degree in control science and engineering from Qufu Normal University, Rizhao, China, in 2008 and 2013, respectively, and the Ph.D. degree in control theory and control engineering from Northeastern University, Shenyang, China, in 2016.

He is currently with the School of Engineering, Qufu Normal University. He was a Visiting Scholar with the Department of Electrical Engineering, Yeungnam University, Gyeongsan, South Korea, in 2017 and 2019, respectively. From 2019 to 2020, he visited the Department of Mechanical Engineering, University of Hong Kong, Hong Kong. His research interests include Markov jump systems, switched systems, positive systems, and networked control systems.

Dr. Qi is an Associate Editor for *International Journal of Control, Automation, and Systems*.

Ning Zhang received the B.S. degree in mathematics in 2019 from Liaocheng University, Liaocheng, China, where she is currently working toward the M.S. degree in operational research and cybernetics.

Her current research interests include stochastic switched systems, networked control systems, and sliding mode control.

Ju H. Park (Senior Member, IEEE) received the Ph.D. degree in electronics and electrical engineering from the Pohang University of Science and Technology (POSTECH), Pohang, South Korea, in 1997.

From May 1997 to February 2000, he was a Research Associate with Engineering Research Center-Automation Research Center, POSTECH. In March 2000, he joined Yeungnam University, Kyongsan, South Korea, where he is currently the Chuma Chair Professor. He has coauthored monographs *Recent Advances in Control and Filtering of Dynamic Systems with Constrained Signals* (Springer-Nature, 2018) and *Dynamic Systems With Time Delays: Stability and Control* (Springer-Nature, 2019), and the Editor of an edited volume *Recent Advances in Control Problems of Dynamical Systems and Networks* (Springer-Nature, 2020). He has authored or coauthored a number of articles in the areas of his research interests, which include robust control and filtering, neural/complex networks, fuzzy systems, multiagent systems, and chaotic systems.

Dr. Park has been the recipient of the Highly Cited Researchers Award by Clarivate Analytics (formerly, Thomson Reuters) since 2015, and listed in three fields, engineering, computer sciences, and mathematics, in 2019–2022. He is the Subject Editor/Advisory Editor/Associate Editor/Editorial Board Member of several international journals, including *IET Control Theory & Applications, Applied Mathematics and Computation, Journal of The Franklin Institute, Nonlinear Dynamics, Engineering Reports, Cogent Engineering*, IEEE TRANSACTION ON FUZZY SYSTEMS, IEEE TRANSACTION ON NEURAL NETWORKS AND LEARNING SYSTEMS, and IEEE TRANSACTION ON CYBERNETICS. He is a Fellow of the Korean Academy of Science and Technology.

Hak-Keung Lam (Fellow, IEEE) received the B.Eng. (Hons.) degree in electronic engineering and the Ph.D. degree in electronic and information engineering from the Department of Electronic and Information Engineering, Hong Kong Polytechnic University, Hong Kong, in 1995 and 2000, respectively.

During 2000–2005, he was a Postdoctoral Fellow and a Research Fellow with the Department of Electronic and Information Engineering, Hong Kong Polytechnic University. He joined as a Lecturer with Kings College London, London, U.K., in 2005 and is currently a Reader. He has authored or coauthored three monographs: *Stability Analysis of Fuzzy-Model-Based Control Systems* (Springer, 2011), *Polynomial Fuzzy Model Based Control Systems* (Springer, 2016), and *Analysis and Synthesis for Interval Type-2 Fuzzy- Model-Based Systems* (Springer, 2016). His current research interests include intelligent control, computational intelligence, and machine learning.

Dr. Lam was a Program Committee Member, an International Advisory Board Member, the Invited Session Chair, and the Publication Chair for various international conferences and a Reviewer for various books, international journals, and international conferences. He was an Associate Editor for IEEE TRANSACTIONS ON CIRCUITS AND SYSTEMS II: EXPRESS BRIEFS, and is currently an Associate Editor for IEEE TRANSACTIONS ON FUZZY SYSTEMS, *IET Control Theory and Applications*, *International Journal of Fuzzy Systems*, *Neurocomputing*, and *Nonlinear Dynamics*, and the Guest Editor for a number of international journals. He is currently on the Editorial Board of the *Journal of Intelligent Learning Systems and Applications*, *Journal of Applied Mathematics*, *Mathematical Problems in Engineering*, *Modeling and Simulation in Engineering*, *Annual Review of Chaos Theory*, *Bifurcations and Dynamical System*, *The Open Cybernetics and Systemics Journal*, *Cogent Engineering*, and *International Journal of Sensors, Wireless Communications and Control*. He was named as a highly cited Researcher. He is the Co-Editor of two edited volumes: *Control of Chaotic Nonlinear Circuits* (World Scientific, 2009) and *Computational Intelligence and Its Applications* (World Scientific, 2012).

Jun Cheng received the B.S. degree in mathematics and applied mathematics from the Hubei University for Nationalities, Enshi, China, in 2010, and the Ph.D. degree in instrumentation science and technology from the University of Electronic Science and Technology of China, Chengdu, China, in 2015.

He is currently with Guangxi Normal University, Guilin, China. From 2013 to 2014, he was a Visiting Scholar with the Department of Electrical and Computer Engineering, National University of Singapore, Singapore. In 2016 and 2018, he was a Visiting Scholar with the Department of Electrical Engineering, Yeungnam University, Gyeongsan, South Korea. His current research interests include analysis and synthesis for stochastic hybrid systems, networked control systems, robust control, and nonlinear systems.

Dr. Cheng is currently an Associate Editor for *International Journal of Control, Automation, and Systems*.